Received: 23 March 2022 | Revised: 31 May 2022 | Accepted: 26 August 2022

DOI: 10.1002/acs.3503

RESEARCH ARTICLE

WILEY

Controller design for nonlinear systems subject to both input saturation and asymmetry time-varying state constraints: A novel network-based approach

Na Li[1] | **Shan-Liang Zhu**[1,2] | **Wen-Jing He**[1] | **Yu-Qun Han**[1,2]

[1]School of Mathematics and Physics, Qingdao University of Science and Technology, Qingdao, China

[2]Research Institute for Mathematics and Interdisciplinary Sciences, Qingdao University of Science and Technology, Qingdao, China

Correspondence
Yu-Qun Han, School of Mathematics and Physics, Qingdao University of Science and Technology, Qingdao 266061, China.
Email: yuqunhan@163.com

Funding information
Shandong Provincial Natural Science Foundation, China, Grant/Award Number: ZR2020QF055

Summary

In this article, the issues of asymmetric input saturation and asymmetric time-varying state constraints are integrated into nonlinear systems for the first time, and a new adaptive tracking control strategy is proposed based on the multi-dimensional Taylor network (MTN) method. Firstly, by introducing a continuous auxiliary function, the input saturation is transformed into a smooth model with bounded error. Secondly, MTNs are employed to estimate nonlinear functions, asymmetric barrier Lyapunov functions (ABLFs) are constructed to make all state variables meet asymmetric constraints, and then a novel control scheme with simple structure is developed via backstepping. Thirdly, according to the Lyapunov stability theory, it is proved that all signals in the closed-loop systems are bounded, and all state variables do not violate the constraints. Finally, three examples show the effectiveness of the proposed scheme.

KEYWORDS

adaptive control, input saturation, multi-dimensional Taylor network, nonlinear systems, state constraints

1 | INTRODUCTION

In recent decades, since nonlinear phenomena is inevitable in the field of practical engineering, nonlinear systems have been greatly developed.[1-3] With the continuous development of science and technology, various effective control schemes have been proposed gradually, such as feedback control,[4-6] sliding mode control,[7] adaptive control,[8,9] fault-tolerant control,[10,11] backstepping control[12] and linear matrix inequality.[13] In these methods, adaptive control technology is an important method to deal with the control problem of nonlinear systems because it is especially suitable for dealing with unknown nonlinearity.

In fact, due to the complexity and diversity of nonlinear systems, any single control method cannot achieve satisfactory performance. Therefore, it is of great theoretical and practical significance to combine different control methods. In particular, by combining adaptive control technology and intelligent control technology, a large number of control methods have been proposed, such as neural networks (NNs)-based control,[14-16] fuzzy logic systems (FLSs)-based control.[17-20] In recent years, multi-dimensional Taylor network (MTN), a novel NN with special structure, has been proposed to solve the control problem of nonlinear systems and many meaningful results have been obtained for general nonlinear systems,[21,22] single-in single-out nonlinear systems,[23,24] multiple-input multiple-output nonlinear systems,[25,26] nonlinear input-delay systems,[27] etc. Although many developments have been achieved for nonlinear systems based on MTN technology, most of the above results ignored the existence of constraints, including input constraints and state

constraints. So, it is important to further study nonlinear systems with full state constraints and input saturation based on MTN.

On one hand, increasing attention has been paid on nonlinear systems with state constraints due to the needs of engineering. Since the violation of state constraints may result in reduced the control effect and even destroyed the stability of the system, and various effective methods have been gradually proposed.[28,29] In particular, the barrier Lyapunov functions (BLFs) method has become an important method to solve the problem of state constraints, and a series of effective adaptive tracking control approaches have been developed, and many types of BLFs have been proposed, such as logarithmic BLFs,[30-32] integral BLFs,[9] tangent BLFs[33,34] and the like. In addition, for the issue of asymmetric time-varying full state constraints, the asymmetric barrier Lyapunov functions (ABLFs) were introduced in Reference 35 for a class of nonlinear systems. This method has been applied to pure feedback nonlinear systems,[36] time-varying delay nonlinear systems,[29] finite-time nonlinear systems[37] and so on.

On the other hand, considering the restrictions of physical limitations and mechanical design, input constraint exists in many practical systems. The existence of input saturation is one of the main causes of instability in the control systems. In order to reduce the influence of input saturation on the system, many control methods have been proposed, such as the compensation method[38,39] and the approximation method.[40,41] Based on the above methods, by combining approximation-based methodology with adaptive backstepping approaches, many control strategies have been developed for nonlinear systems with input saturation.[42-44] However, to the author's knowledge, there are few results devoted to studying the nonlinear systems subject to asymmetric input saturation and asymmetric time-varying full-state constraints under a unified framework, which also urges the study of this paper.

Based on the above results, this paper focuses on the MTN-based tracking control design of nonlinear systems with asymmetric time-varying full state constraints and input saturation. Firstly, an auxiliary smoothing function is introduced to solve the problem of asymmetric input saturation. Secondly, by constructing ABLFs to ensure that all states meet the given constraints, and then, a novel adaptive control strategy with simple structure is designed via backstepping with the help of the approximation performance of MTN. The main contributions of this paper are as follows:

(1) The MTN technology is integrated into the nonlinear system with time-varying full state constraints and input saturation for the first time. For the sake of dealing with the problem of asymmetric full-state constraints, ABLFs is used to avoid the constraint exceeding the limit, and a MTN is employed to approximate the unknown nonlinearity in the system, so a simple MTN adaptive controller is designed, and the designed control scheme has good tracking effect and practicability.
(2) For nonlinear systems with time-varying full state constraints, the problem of input saturation is rarely studied at the same time. For the nonlinear systems and stochastic nonlinear systems, although the authors in References 28,45,46 have studied the systems with full state constraints and input saturation, these results focus on general symmetric constant constraints rather than asymmetric time-varying full state constraints. Despite the asymmetric time-varying full-state constraints problem has been considered in References 35-37, the research on input saturation was ignored. In addition, compared with the non-strict feedback nonlinear systems with full-state constraints,[47] the problems studied in this paper are broader and the systems considered is more general.
(3) The MTN-based control method proposed in this paper has the advantages of simple structure and good approximation effect. Despite that many developments have been developed for nonlinear systems with asymmetric input saturation,[48-50] the above control methods were only suitable for asymmetric constant input saturation rather than asymmetric time-varying full state constraints. It is of interest to note that the previous results[34,51] only focused on the nonlinear systems with input dead-zone constraints. Therefore, they cannot be applied to the control problems in this paper.

2 | PROBLEM FORMULATION

2.1 | Problem description

In this paper, the following form of nonlinear system is considered

$$\begin{cases} \dot{x}_i = x_{i+1} + f_i\left(\bar{x}_i\right), i = 1, \ldots, n-1 \\ \dot{x}_n = u(v) + f_n\left(\bar{x}_n\right) \\ y = x_1 \end{cases}, \tag{1}$$

where $x_1, x_2, \ldots, x_n$ denote the system states with $\bar{x}_i = [x_1, \ldots, x_i]^{\mathrm{T}} \in \mathbb{R}^i$, for $i = 1, \ldots, n$. $y \in \mathbb{R}$ represents the output of the system and $f_i : \mathbb{R}^i \to \mathbb{R}$ is uncertain nonlinear continuous function. In addition, $u(v) \in \mathbb{R}$ denotes the output of input saturation, which can be described by the following asymmetric saturation model

$$u(v) = \begin{cases} u_I, & v \le u_I \\ v, & u_I < v < u_S \\ u_S, & v \ge u_S \end{cases}, \tag{2}$$

where v denotes the input signal with saturation nonlinearity, u_I and u_S are the supremum and infimum that the $u(v)$ can take, respectively.

Remark 1. It should be noted that the existence of input saturation often result in system instability. Therefore, it is an important research direction to design a reasonable controller to eliminate or reduce the impact of input constraints on system performance. The model (2) clearly shows that the mathematical description of the input saturation constraint is discontinuous, and there are two sharp angles when $v = u_I$ and $v = u_S$. As a result, the backstepping design method cannot be used to construct control signals directly. To overcome this problem, approximation-based method will be used to eliminate the influence of saturation nonlinearity on the system.

For the nonlinear system (1), the main task of this study is to develop an adaptive control strategy ensure that

(1) Every state $x_i\,(i = 1, \ldots, n)$ falls into its given set $\Omega_{x_i} = \left\{x_i \middle| b_i^-(t) < x_i < b_i^+(t), b_i^{\pm}(t) : \mathbb{R}^+ \to \mathbb{R}^+\right\}$, where $b_i^-(t) < b_i^+(t)$ for $i = 1, 2, \ldots, n$.
(2) The system output y can follow the desired reference signal y_d.

In order to achieve the control objectives better, the following assumptions are needed:

Assumption 1 (34). The reference signal y_d and its derivative up to nth with respect to time t are continuous and bounded.

Assumption 2 (34). For the reference signal y_d and its ith time derivative $y_d^{(i)}$, there exist functions $Y_i(t) : \mathbb{R}^+ \to \mathbb{R}^+, i = 0, 1, 2, \ldots n-1$ satisfy $\underline{Y}_0(t) \leqslant y_d \leqslant \overline{Y}_0(t)$ and $\left|y_d^{(i)}\right| \leqslant Y_i$, where $\overline{Y}_0$ and $\underline{Y}_0$ are the upper and lower bounds of Y_0.

Remark 2. The Assumption 1 means that the reference signal y_d can be used for controller design, which is commonly considered in the tracking control problem of nonlinear systems. The Assumption 2 is a standard assumption condition adopted widely in the full-state constraints,[9,34] which is helpful for the controller design for the problem of full-state constraints of nonlinear systems.

Remark 3. It is noted that the results given in References 28,45,46 are only focus on the nonlinear systems with full state constraints. Different from References 28,45,46, the existence of asymmetric time-varying full state constraints causes much difficulty for the analysis and synthesis of nonlinear systems. Therefore, the control issue considered in this paper is more representative. In addition, it is worth noting that for the asymmetric time-varying full state constraints considered in this paper, the asymmetric time-varying BLFs are selected in the backstepping process, which can not only solve the case of constant constraints, but also the case of time-varying constraints.

2.2 | Knowledge preparation

As described in Reference 30, for the sake of eliminating the impact of input saturation, a continuous function $\Xi(x)$ is introduced to obtain the following saturation model in order to approximate the saturation nonlinearity in the system

$$u(v) = \bar{u} \cdot \Xi\left(\frac{\sqrt{\pi}}{2\bar{u}} v\right), \tag{3}$$

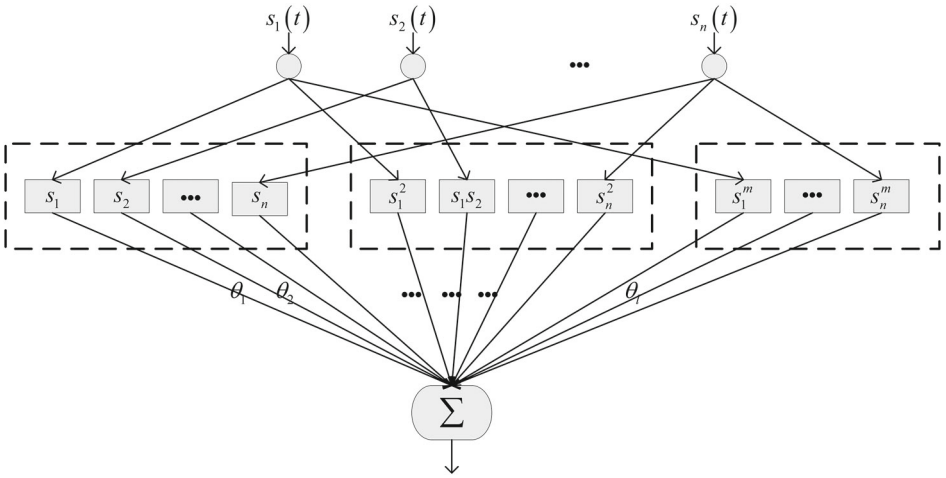

FIGURE 1 The structure diagram of MTN

where $\bar{u} = \left(u_S + \frac{1}{2}u_I\right) + \left(u_S - \frac{1}{2}u_I\right) sign(v)$, and $\Xi(\cdot)$ is a Gaussian error function define as $\Xi(x) = \frac{2}{\sqrt{\pi}}\int_0^x e^{-s^2} ds$.

For the convenience, define a function as $e(v) = u - \ell v$. Then, (3) can be expressed as form $u = \ell v + e(v)$, where $\ell > 0$ is a constant.

Assumption 3 (52). There exist constants $\Delta > 0$, ℓ^- and ℓ^+, such that $e(v) \leq \Delta$ and $\ell \in \left[\ell^-, \ell^+\right]$.

Remark 4. It must be said that $e(v)$ is bounded in Assumption 3 is reasonable from the practical point of view, which is commonly adopted in the literature.[52,53] Furthermore, the boundaries of Δ, ℓ^- and ℓ^+ are only used for stability analysis and are not required in the controller design.

Lemma 1 (32). *For $\forall z \in \mathbb{R}$ and $\forall k_c \in \mathbb{R}^+$, if $|z| < k_c$, the following inequality holds:*

$$\ln \frac{k_c^{2q}}{k_c^{2q} - z^{2q}} < \frac{z^{2q}}{k_c^{2q} - z^{2q}} \tag{4}$$

where $\ln(\cdot)$ is the logarithmic of $\cdot$, and q is a positive integer.

2.3 | Multi-dimensional Taylor network

As shown in Figure 1, MTN is a three-layer feedforward neural network, including input layer, middle layer and output layer. Considering that the concept and structure of MTN have been introduced in the recent work,[21,22,26,27,54] only the following lemma is stated for function approximation.

Lemma 2 (30). *For a continuous function $f(\boldsymbol{S})$ defined on a compact set Ω, it can be approximated by a MTN with any given accuracy $\varepsilon > 0$. Namely,*

$$f(\boldsymbol{S}) = \boldsymbol{\theta}^{*\mathrm{T}} P_{m_n}(\boldsymbol{S}) + \gamma(\boldsymbol{S}),\ |\gamma(\boldsymbol{S})| < \varepsilon, \tag{5}$$

where $\boldsymbol{S} = [s_1, \ldots, s_n]^{\mathrm{T}} \in \mathbb{R}^n$ is the input vector, $P_{m_n}(\boldsymbol{S}) = \left[s_1, \ldots, s_n, s_1^2, s_1s_2, \ldots, s_1s_n, s_2s_3, \ldots, s_n^2, s_1^m, \ldots, s_n^m\right]^{\mathrm{T}} \in \mathbb{R}^l$ denotes the intermediate layer, which is made up of the polynomial combination of input vector. $\boldsymbol{\theta}^* = \left[\theta_1^*, \ldots, \theta_l^*\right]^{\mathrm{T}} \in \mathbb{R}^l$ denotes the ideal weight vector and defined as $\boldsymbol{\theta}^* := \arg\min_{\theta \in \mathbb{R}^l} \left\{ \sup_{\boldsymbol{S} \in \Omega} \left| f(\boldsymbol{S}) - \boldsymbol{\theta}^{\mathrm{T}} P_{m_n}(\boldsymbol{S}) \right| \right\}$.

3 | MAIN RESULTS

3.1 | Controller design

Define the intermediate variables $z_1 = x_1 - y_d$ and $z_i = x_i - \alpha_{i-1}$, $i = 2, 3, \ldots, n$, where α_{i-1} is intermediate virtual signals, which will be designed later.

Step 1: Combining $z_1 = x_1 - y_d$ with the first equation in system (1), one has

$$\dot{z}_1 = x_2 + f_1 - \dot{y}_d, \tag{6}$$

Then, considering the asymmetric time-varying BLF as follows

$$V_1 = \frac{\rho(z_1)}{2}\ln\left(\frac{k_{b1}^2(t)}{k_{b1}^2(t) - z_1^2}\right) + \frac{1-\rho(z_1)}{2}\ln\left(\frac{k_{a1}^2(t)}{k_{a1}^2(t) - z_1^2}\right) + \frac{1}{2}\tilde{\theta}_1^{\mathrm{T}}\tilde{\theta}_1, \tag{7}$$

where $\tilde{\theta}_1 = \theta_1 - \hat{\theta}_1$ is the parameter error, $k_{a1}(t) = b_1^-(t) - y_d$, $k_{b1}(t) = b_1^+(t) - y_d$ and $\rho(z_1) = \begin{cases} 1, & z_1 \geq 0 \\ 0, & z_1 < 0 \end{cases}$.

Remark 5. For the convenience of later calculation, the variable t will be omitted.

Then, calculating the derivative of V_1 with respect to time t in $\Theta_{z_1} = \{z_1 : |k_{a1} \leqslant z_1 \leqslant k_{b1}\}$, one has

$$\begin{aligned}\dot{V}_1 &= \frac{\rho_1(z_1)}{k_{b1}}\frac{\dot{k}_{b1}\left(k_{b1}^2 - z_1^2\right) - k_{b1}\left(k_{b1}\dot{k}_{b1} - z_1\dot{z}_1\right)}{\left(k_{b1}^2 - z_1^2\right)} + \frac{1-\rho_1(z_1)}{k_{a1}}\frac{\dot{k}_{a1}\left(k_{a1}^2 - z_1^2\right) - k_{a1}\left(k_{a1}\dot{k}_{a1} - z_1\dot{z}_1\right)}{\left(k_{a1}^2 - z_1^2\right)} - \tilde{\theta}_1^{\mathrm{T}}\dot{\hat{\theta}}_1 \\ &= \rho_1(z_1)\left(\frac{\dot{k}_{b1}}{k_{b1}} - \frac{k_{b1}\dot{k}_{b1} - z_1\dot{z}_1}{k_{b1}^2 - z_1^2}\right) + (1-\rho_1(z_1))\left(\frac{\dot{k}_{a1}}{k_{a1}} - \frac{k_{a1}\dot{k}_{a1} - z_1\dot{z}_1}{k_{a1}^2 - z_1^2}\right) - \tilde{\theta}_1^{\mathrm{T}}\dot{\hat{\theta}}_1\end{aligned} \tag{8}$$

Next, denote $K_{b1} = \frac{z_1}{k_{b1}}$, $K_{a1} = \frac{z_1}{k_{a1}}$ and $\mu_1 = \frac{\rho_1}{k_{b1}^2 - z_1^2} + \frac{1-\rho_1}{k_{a1}^2 - z_1^2}$, (8) can be simplified to the form as follows

$$\begin{aligned}\dot{V}_1 &= \frac{\rho(z_1)K_{b1}}{k_{b1}\left(1 - K_{b1}^2\right)}\left(\dot{z}_1 - \frac{\dot{k}_{b1}}{k_{b1}}z_1\right) + \frac{(1-\rho_1)K_{a1}}{k_{a1}\left(1 - K_{a1}^2\right)}\left(\dot{z}_1 - z_1\frac{\dot{k}_{a1}}{k_{a1}}\right) - \tilde{\theta}_1^{\mathrm{T}}\dot{\hat{\theta}}_1 \\ &= \left(\frac{\rho_1 K_{b1}}{k_{b1}\left(1 - K_{b1}^2\right)} + \frac{(1-\rho_1)K_{a1}}{k_{a1}\left(1 - K_{a1}^2\right)}\right)\dot{z}_1 - \left[\frac{\dot{k}_{b1}}{k_{b1}}\frac{\rho_1 K_{b1}}{k_{b1}\left(1 - K_{b1}^2\right)} + \frac{\dot{k}_{a1}}{k_{a1}}\frac{(1-\rho_1)K_{a1}}{k_{a1}\left(1 - K_{a1}^2\right)}\right]z_1 - \tilde{\theta}_1^{\mathrm{T}}\dot{\hat{\theta}}_1 \\ &= \left(\frac{\rho_1}{k_{b1}^2 - z_1^2} + \frac{1-\rho_1}{k_{a1}^2 - z_1^2}\right)z_1\dot{z}_1 - \left[\frac{\dot{k}_{b1}}{k_{b1}}\frac{\rho_1 K_{b1}}{k_{b1}\left(1 - K_{b1}^2\right)} + \frac{\dot{k}_{a1}}{k_{a1}}\frac{(1-\rho_1)K_{a1}}{k_{a1}\left(1 - K_{a1}^2\right)}\right]z_1 - \tilde{\theta}_1^{\mathrm{T}}\dot{\hat{\theta}}_1 \\ &= \mu_1 z_1\dot{z}_1 - \tilde{\theta}_1^{\mathrm{T}}\dot{\hat{\theta}}_1 - \left[\frac{\dot{k}_{b1}}{k_{b1}}\frac{\rho_1 K_{b1}}{k_{b1}\left(1 - K_{b1}^2\right)} + \frac{\dot{k}_{a1}}{k_{a1}}\frac{(1-\rho_1)K_{a1}}{k_{a1}\left(1 - K_{a1}^2\right)}\right]z_1.\end{aligned} \tag{9}$$

Taking (6) into consideration, (9) can be further expressed as follows

$$\dot{V}_1 = \mu_1 z_1\left(x_2 + \tilde{f}_1\right) - \mu_1^2 z_1^2 - \tilde{\theta}_1^{\mathrm{T}}\dot{\hat{\theta}}_1, \tag{10}$$

where $\tilde{f}_1 = f_1 - \dot{y}_d - \frac{1}{\mu_1}\left(\frac{\dot{k}_{b1}}{k_{b1}}\frac{\rho_1 K_{b1}}{k_{b1}\left(1-K_{b1}^2\right)} + \frac{\dot{k}_{a1}}{k_{a1}}\frac{(1-\rho_1)K_{a1}}{k_{a1}\left(1-K_{a1}^2\right)}\right) + \mu_1 z_1$.

Remark 6. It should be noted that, when $z_1 \geq 0$, $\rho_1 = 1$, then $\frac{1}{\mu_1}\left(\frac{\dot{k}_{b1}}{k_{b1}}\frac{\rho_1 K_{b1}}{k_{b1}\left(1-K_{b1}^2\right)} + \frac{\dot{k}_{a1}}{k_{a1}}\frac{(1-\rho_1)K_{a1}}{k_{a1}\left(1-K_{a1}^2\right)}\right) = \frac{\dot{k}_{b1}}{k_{b1}}z_1$, when $z_1 < 0$, $\rho_1 = 1$, then $\frac{1}{\mu_1}\left(\frac{\dot{k}_{b1}}{k_{b1}}\frac{\rho_1 K_{b1}}{k_{b1}\left(1-K_{b1}^2\right)} + \frac{\dot{k}_{a1}}{k_{a1}}\frac{(1-\rho_1)K_{a1}}{k_{a1}\left(1-K_{a1}^2\right)}\right) = \frac{\dot{k}_{a1}}{k_{a1}}z_1$. Therefore, $\tilde{f}_1$ is a continuous function.

Considering that unknown function $\tilde{f}_1$ cannot be used to construct virtual controller, in the light of Lemma 2, a MTN is employed to approximate $\tilde{f}_1$ with any accuracy $\varepsilon_1 > 0$, that is

$$\tilde{f}_1 = \theta_1^{\mathrm{T}}P_{m_1}(\boldsymbol{Z}_1) + \gamma_1(\boldsymbol{Z}_1), \ |\gamma_1(\boldsymbol{Z}_1)| \leq \varepsilon_1, \tag{11}$$

where $\gamma_1(\boldsymbol{Z}_1)$ is approximation error.

Then, substituting (11) into (10), one has

$$\dot{V}_1 = \mu_1 z_1 \left(z_2 + \alpha_1 + \theta_1^{\mathrm{T}} P_{m_1} + \gamma_1\right) - \mu_1^2 z_1^2 - \tilde{\theta}_1^{\mathrm{T}} \dot{\hat{\theta}}_1, \tag{12}$$

On the basis of Young's Inequality, the following inequalities can be obtained

$$\mu_1 z_1 z_2 \leq \frac{1}{2}\mu_1^2 z_1^2 + \frac{1}{2} z_2^2, \tag{13}$$

$$\mu_1 z_1 \gamma_1 \leq \frac{1}{2}\mu_1^2 z_1^2 + \frac{1}{2}\varepsilon_1^2. \tag{14}$$

Substituting (13) and (14) into (12), the following inequality holds

$$\dot{V}_1 \leq \mu_1 z_1 \left(\alpha_1 + \theta_1^{\mathrm{T}} P_{m_1}\right) + \frac{1}{2} z_2^2 + \frac{1}{2}\varepsilon_1^2 - \tilde{\theta}_1^{\mathrm{T}} \dot{\hat{\theta}}_1. \tag{15}$$

Based on (15), the first intermediate virtual control signal α_1 can be constructed as follows

$$\alpha_1 = -\kappa_1 z_1 - \hat{\theta}_1^{\mathrm{T}} P_{m_1}, \tag{16}$$

where $\kappa_1 > 0$ is a design constant.

Then, substituting (16) into (15), the following inequality can be obtained

$$\begin{aligned} \dot{V}_1 &\leq \mu_1 z_1 \left(-\kappa_1 z_1 - \hat{\theta}_1^{\mathrm{T}} P_{m_1} + \theta_1^{\mathrm{T}} P_{m_1}\right) + \frac{1}{2} z_2^2 + \frac{1}{2}\varepsilon_1^2 - \tilde{\theta}_1^{\mathrm{T}} \dot{\hat{\theta}}_1 \\ &= -\kappa_1 \mu_1 z_1^2 + \frac{1}{2} z_2^2 + \tilde{\theta}_1^{\mathrm{T}} \left(\mu_1 z_1 P_{m_1} - \dot{\hat{\theta}}_1\right) + \frac{1}{2}\varepsilon_1^2. \end{aligned} \tag{17}$$

Step i $(2 \leq i \leq n-1)$: Combining $z_i = x_i - \alpha_{i-1}$ with the ith equation in system (1), one has

$$\dot{z}_i = x_{i+1} + f_i - \dot{\alpha}_{i-1}. \tag{18}$$

Then, considering the asymmetric time-varying BLF as follows

$$V_i = V_{i-1} + \frac{\rho(z_i)}{2} \ln\left(\frac{k_{bi}^2}{k_{bi}^2 - z_i^2}\right) + \frac{1-\rho(z_i)}{2} \ln\left(\frac{k_{ai}^2}{k_{ai}^2 - z_i^2}\right) + \frac{1}{2}\tilde{\theta}_i^{\mathrm{T}} \tilde{\theta}_i, \tag{19}$$

where $\tilde{\theta}_i = \theta_i - \hat{\theta}_i$ is the error vector of parameter estimation, $k_{ai} = b_i^- - Y_{i-1}$, $k_{bi} = b_i^+ - Y_{i-1}$, and $\rho(z_i) = \begin{cases} 1, & z_i \geq 0 \\ 0, & z_i < 0 \end{cases}$.

Based on Mathematical Induction method, the following formulas can be summarized

$$\dot{V}_{i-1} \leq -\sum_{j=1}^{i-1} \kappa_j \mu_j z_j^2 + \frac{1}{2} z_i^2 + \sum_{j=1}^{i-1} \tilde{\theta}_j^{\mathrm{T}} \left(\mu_j z_j P_{m_j} - \dot{\hat{\theta}}_j\right) + \frac{1}{2}\sum_{j=1}^{i-1} \varepsilon_j^2, \tag{20}$$

where $\kappa_j > 0$ is a positive constant.

Calculating the derivative of V_i with respect to time t in $\Theta_{z_i} = \{z_i : |k_{ai} \leqslant z_i \leqslant k_{bi}\}$, and denote $K_{bi} = \frac{z_i}{k_{bi}}$, $K_{ai} = \frac{z_i}{k_{ai}}$, and $\mu_i = \frac{\rho_i}{k_{bi}^2 - z_i^2} + \frac{1-\rho_i}{k_{ai}^2 - z_i^2}$, we have

$$\begin{aligned} \dot{V}_i &= \dot{V}_{i-1} + \frac{\rho_i(z_i)}{k_{bi}} \frac{\dot{k}_{bi}\left(k_{bi}^2 - z_i^2\right) - k_{bi}\left(k_{bi}\dot{k}_{bi} - z_i \dot{z}_i\right)}{\left(k_{bi}^2 - z_i^2\right)} + \frac{1-\rho_i(z_i)}{k_{ai}} \frac{\dot{k}_{ai}\left(k_{ai}^2 - z_i^2\right) - k_{ai}\left(k_{ai}\dot{k}_{ai} - z_i \dot{z}_i\right)}{\left(k_{ai}^2 - z_i^2\right)} - \tilde{\theta}_i^{\mathrm{T}} \dot{\hat{\theta}}_i \\ &= \dot{V}_{i-1} + \mu_i z_i \dot{z}_i - \tilde{\theta}_i^{\mathrm{T}} \dot{\hat{\theta}}_i - \left[\frac{\dot{k}_{bi}}{k_{bi}} \frac{\rho_i K_{bi}}{k_{bi}\left(1 - K_{bi}^2\right)} + \frac{\dot{k}_{ai}}{k_{ai}} \frac{(1-\rho_i) K_{ai}}{k_{ai}\left(1 - K_{ai}^2\right)}\right] z_i. \end{aligned} \tag{21}$$

Substituting (18) into (21), then (21) can be rewritten as follows

$$\begin{aligned}\dot{V}_i &= \dot{V}_{i-1} + \mu_i z_i \left(x_{i+1} + f_i - \dot{\alpha}_{i-1}\right) - \left[\frac{\dot{k}_{bi}}{k_{bi}} \frac{\rho_1 K_{bi}}{k_{bi}\left(1-K_{bi}^2\right)} + \frac{\dot{k}_{ai}}{k_{ai}} \frac{(1-\rho_i) K_{ai}}{k_{ai}\left(1-K_{ai}^2\right)}\right] z_i - \tilde{\theta}_i^{\mathrm{T}} \dot{\hat{\theta}}_i \\ &= \dot{V}_{i-1} + \mu_i z_i \left(x_{i+1} + \tilde{f}_i\right) - \frac{1}{2} z_i^2 - \mu_i^2 z_i^2 - \tilde{\theta}_i^{\mathrm{T}} \dot{\hat{\theta}}_i, \end{aligned} \tag{22}$$

where $\tilde{f}_i = f_i - \dot{\alpha}_{i-1} - \frac{1}{\mu_i}\left(\frac{\dot{k}_{bi}}{k_{bi}} \frac{\rho_1 K_{bi}}{k_{bi}\left(1-K_{bi}^2\right)} + \frac{\dot{k}_{ai}}{k_{ai}} \frac{(1-\rho_i) K_{ai}}{k_{ai}\left(1-K_{ai}^2\right)}\right) + \mu_i z_i + \frac{1}{2\mu_i} z_i$.

Considering that the unknown nonlinear function $\tilde{f}_i$ cannot be used to construct virtual controller, according to Lemma 2, a MTN is employed to approximate $\tilde{f}_i$ with any accuracy $\varepsilon_i > 0$, that is

$$\tilde{f}_i = \theta_i^{\mathrm{T}} P_{m_i}(\boldsymbol{Z}_i) + \gamma_i(\boldsymbol{Z}_i), \ |\gamma_i(\boldsymbol{Z}_i)| \le \varepsilon_i, \tag{23}$$

where $\gamma_i(\boldsymbol{Z}_1)$ is approximation error.

Substituting (23) into (22), the following inequality can be obtained

$$\begin{aligned}\dot{V}_i &= \dot{V}_{i-1} + \mu_i z_i \left(x_{i+1} + \tilde{f}_i\right) - \frac{1}{2} z_i^2 - \mu_i^2 z_i^2 - \tilde{\theta}_i^{\mathrm{T}} \dot{\hat{\theta}}_i \\ &= \dot{V}_{i-1} + \mu_i z_i \left(z_{i+1} + \alpha_i + \theta_i^{\mathrm{T}} P_{m_i} + \gamma_i\right) - \frac{1}{2} z_i^2 - \mu_i^2 z_i^2 - \tilde{\theta}_i^{\mathrm{T}} \dot{\hat{\theta}}_i. \end{aligned} \tag{24}$$

By exploiting Young's Inequality, the following two inequalities are easily obtained

$$\mu_i z_i z_{i+1} \le \frac{1}{2} \mu_i^2 z_i^2 + \frac{1}{2} z_{i+1}^2, \tag{25}$$

$$\mu_i z_i \gamma_i \le \frac{1}{2} \mu_i^2 z_i^2 + \frac{1}{2} \varepsilon_i^2. \tag{26}$$

Using inequalities (25) and (26), (24) can be expressed in the following form

$$\begin{aligned}\dot{V}_i &= \dot{V}_{i-1} + \mu_i z_i \left(z_{i+1} + \alpha_i + \theta_i^{\mathrm{T}} P_{m_i} + \gamma_i\right) - \frac{1}{2} z_i^2 - \mu_i^2 z_i^2 - \tilde{\theta}_i^{\mathrm{T}} \dot{\hat{\theta}}_i \\ &\le \dot{V}_{i-1} + \mu_i z_i \left(\alpha_i + \theta_i^{\mathrm{T}} P_{m_i}\right) + \frac{1}{2} z_{i+1}^2 - \frac{1}{2} z_i^2 + \frac{1}{2} \varepsilon_i^2 - \tilde{\theta}_i^{\mathrm{T}} \dot{\hat{\theta}}_i. \end{aligned} \tag{27}$$

According to (27), designing the ith intermediate virtual signal α_i as follows

$$\alpha_i = -\kappa_i z_i - \hat{\theta}_i^{\mathrm{T}} P_{m_i} \tag{28}$$

where $\kappa_i > 0$ is a design constant.

Substituting (20) and (28) into (27), the following formula can be proved to be correct

$$\dot{V}_i \le -\sum_{j=1}^{i} \kappa_j \mu_j z_j^2 + \frac{1}{2} z_{i+1}^2 + \sum_{j=1}^{i} \tilde{\theta}_j^{\mathrm{T}} \left(\mu_j z_j P_{m_j} - \dot{\hat{\theta}}_j\right) + \frac{1}{2} \sum_{j=1}^{i} \varepsilon_j^2. \tag{29}$$

Step n: Combining $z_n = x_n - \alpha_{n-1}$ with $u = \ell v + e(v)$, one has

$$\dot{z}_n = \ell v + e(v) + f_n - \dot{\alpha}_{n-1}. \tag{30}$$

Considering the following asymmetric time-varying BLF as

$$V_n = V_{n-1} + \frac{\rho(z_n)}{2} \ln\left(\frac{k_{bn}^2}{k_{bn}^2 - z_n^2}\right) + \frac{1-\rho(z_n)}{2} \ln\left(\frac{k_{an}^2}{k_{an}^2 - z_n^2}\right) + \frac{1}{2} \tilde{\theta}_n^{\mathrm{T}} \tilde{\theta}_n, \tag{31}$$

where $\tilde{\theta}_n = \theta_n - \hat{\theta}_n$ is the error vector of parameter estimation, $k_{an}(t) = b_n^- - Y_{n-1}$, $k_{bn}(t) = b_n^+ - Y_{n-1}$, and $\rho(z_n) = \begin{cases} 1, & z_n \geq 0 \\ 0, & z_n < 0 \end{cases}$.

Then, similar to the previous steps, we can calculate the derivative of V_n with respect to time t in $\Theta_{z_n} = \{z_n : |k_{an} \leqslant z_n \leqslant k_{bn}\}$, and denote $K_{bn} = \frac{z_n}{k_{bn}}$, $K_{an} = \frac{z_n}{k_{an}}$ and $\mu_n = \frac{\rho_n}{k_{bn}^2 - z_n^2} + \frac{1-\rho_n}{k_{an}^2 - z_n^2}$, we have

$$\dot{V}_n = \dot{V}_{n-1} + \mu_n z_n \dot{z}_n - \left[\frac{\dot{k}_{bn}}{k_{bn}} \frac{\rho K_{bn}}{k_{bn}\left(1 - K_{bn}^2\right)} + \frac{\dot{k}_{an}}{k_{an}} \frac{(1-\rho) K_{an}}{k_{an}\left(1 - K_{an}^2\right)} \right] z_n - \tilde{\theta}_n^{\mathrm{T}} \dot{\hat{\theta}}_n. \tag{32}$$

Substituting (30) into (32), one has

$$\dot{V}_n = \dot{V}_{n-1} + \mu_n z_n \left(\ell v + e(v) + \tilde{f}_n \right) - \frac{1}{2} z_n^2 - \mu_n^2 z_n^2 - \tilde{\theta}_n^{\mathrm{T}} \dot{\hat{\theta}}_n, \tag{33}$$

where $\tilde{f}_n = f_n - \dot{\alpha}_{n-1} - \frac{1}{\mu_n} \left(\frac{\dot{k}_{bn}}{k_{bn}} \frac{\rho K_{bn}}{k_{bn}\left(1-K_{bn}^2\right)} + \frac{\dot{k}_{an}}{k_{an}} \frac{(1-\rho) K_{an}}{k_{an}\left(1-K_{an}^2\right)} \right) + \mu_n z_n + \frac{1}{2\mu_n} z_n$.

Using Young's Inequality, it can be verified that the following inequality is correct

$$\mu_n z_n e(v) \leq \frac{1}{2} \mu_n^2 z_n^2 + \frac{1}{2} \Delta^2. \tag{34}$$

Then, substituting (34) into (33) to get the following formula

$$V_n = \dot{V}_{n-1} + \mu_n z_n \left(\ell v + \tilde{f}_n \right) - \frac{1}{2} z_n^2 - \frac{1}{2} \mu_n^2 z_n^2 + \frac{1}{2} \Delta^2 - \tilde{\theta}_n^{\mathrm{T}} \dot{\hat{\theta}}_n. \tag{35}$$

According to Lemma 2, for any accuracy $\varepsilon_n > 0$, the unknown function $\tilde{f}_n$ can be approximated by a MTN structure with the form of $\boldsymbol{\theta}_n^{\mathrm{T}} P_{m_n}$, that is

$$\tilde{f}_n = \boldsymbol{\theta}_n^{\mathrm{T}} P_{m_n}(\boldsymbol{Z}_n) + \gamma_n(\boldsymbol{Z}_n), \ |\gamma_n(\boldsymbol{Z}_n)| \leq \varepsilon_n, \tag{36}$$

where $\gamma_n(\boldsymbol{Z}_n)$ is approximation error.

Then, substituting (36) into (35), the following formula is easy to hold

$$\dot{V}_n = \dot{V}_{n-1} + \mu_n z_n \left(\ell v + \boldsymbol{\theta}_n^{\mathrm{T}} P_{m_n} + \gamma_n \right) - \frac{1}{2} z_n^2 - \frac{1}{2} \mu_n^2 z_n^2 + \frac{1}{2} \Delta^2 - \tilde{\theta}_n^{\mathrm{T}} \dot{\hat{\theta}}_n. \tag{37}$$

Further, on the basis of Young's Inequality, the following inequalities can be obtained

$$\mu_n z_n \gamma_n \leq \frac{1}{2} \mu_n^2 z_n^2 + \frac{1}{2} \varepsilon_n^2. \tag{38}$$

Consequently, (37) can be expressed as follows

$$\dot{V}_n \leq \dot{V}_{n-1} + \mu_n z_n \left(\ell v + \boldsymbol{\theta}_n^{\mathrm{T}} P_{m_n} \right) + \frac{1}{2} \varepsilon_n^2 - \frac{1}{2} z_n^2 + \frac{1}{2} \Delta^2 - \tilde{\theta}_n^{\mathrm{T}} \dot{\hat{\theta}}_n. \tag{39}$$

According to (39), designing the actual control input v as follows

$$v = -\frac{1}{\ell^-} \left(\kappa_n |z_n| + \left| \hat{\boldsymbol{\theta}}_n^{\mathrm{T}} P_{m_n} \right| \right) \operatorname{sgn}(z_n), \tag{40}$$

where $\kappa_n > 0$ is a design constant.

According to inequality (29), we can get the following formula

$$\dot{V}_{n-1} \leq -\sum_{j=1}^{n-1} \kappa_j \mu_j z_j^2 + \frac{1}{2} z_n^2 + \sum_{j=1}^{n-1} \tilde{\theta}_j^{\mathrm{T}} \left(\mu_j z_j P_{m_j} - \dot{\hat{\theta}}_j \right) + \frac{1}{2} \sum_{j=1}^{n-1} \varepsilon_j^2. \tag{41}$$

Substituting (40) and (41) into (39), the following inequality holds

$$\dot{V}_n \le -\sum_{j=1}^{n}\kappa_j\mu_j z_j^2 + \sum_{j=1}^{n}\tilde{\theta}_j^{\mathrm{T}}\left(\mu_j z_j P_{m_j} - \dot{\hat{\theta}}_j\right) + \frac{1}{2}\sum_{j=1}^{n}\varepsilon_j^2 + \frac{1}{2}\Delta^2. \tag{42}$$

Then we can design the adaptive law according to (42) as follows

$$\dot{\hat{\theta}}_j = -\varpi_j\hat{\theta}_j + \mu_j z_j P_{m_j}, \tag{43}$$

where $j = 1, 2, \ldots, n$, and ϖ_j is a positive design parameter.

Substituting (43) into (42), the following inequality holds

$$\dot{V}_n \le -\sum_{j=1}^{n}\kappa_j\mu_j z_j^2 + \sum_{j=1}^{n}\varpi_j\tilde{\theta}_j^{\mathrm{T}}\hat{\theta}_j + \frac{1}{2}\sum_{j=1}^{n}\varepsilon_j^2 + \frac{1}{2}\Delta^2. \tag{44}$$

Since $\mu_j = \frac{\rho_j}{k_{bj}^2 - z_j^2} + \frac{1-\rho_j}{k_{aj}^2 - z_j^2}$, combining with Lemma 1, we can get the time derivative of V_n as follows

$$\begin{aligned}\dot{V}_n &\le -\sum_{j=1}^{n}\kappa_j\left(\rho_j\frac{z_j^2}{k_{bj}^2 - z_j^2} + (1-\rho_j)\frac{z_j^2}{k_{aj}^2 - z_j^2}\right) + \sum_{j=1}^{n}\varpi_j\tilde{\theta}_j^{\mathrm{T}}\hat{\theta}_j + \frac{1}{2}\sum_{j=1}^{n}\varepsilon_j^2 + \frac{1}{2}\Delta^2\\ &\le -\sum_{j=1}^{n}\kappa_j\left(\rho_j\ln\left(\frac{k_{bj}^2}{k_{bj}^2 - z_j^2}\right) + (1-\rho_j)\ln\left(\frac{k_{aj}^2}{k_{aj}^2 - z_j^2}\right)\right) + \sum_{j=1}^{n}\varpi_j\tilde{\theta}_j^{\mathrm{T}}\hat{\theta}_j + \frac{1}{2}\sum_{j=1}^{n}\varepsilon_j^2 + \frac{1}{2}\Delta^2.\end{aligned} \tag{45}$$

In this way, the design of the controller is completed. Figure 2 clearly describes the whole design process.

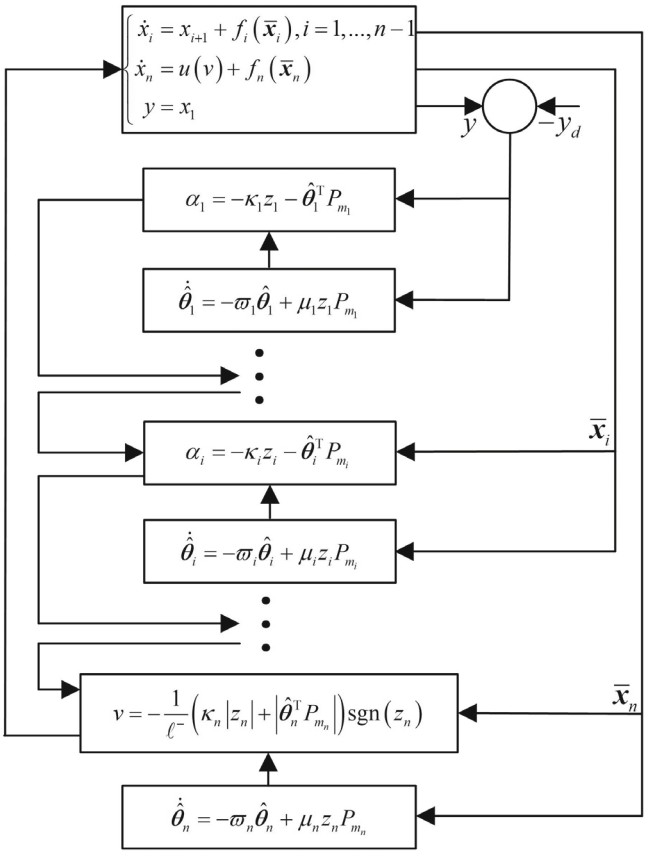

FIGURE 2 Control design process

3.2 | Stability analysis

According to the above work, the main conclusions of this paper can be summarized as follows:

Theorem 1. *Consider nonlinear system (1) with asymmetric time-varying full state constraints and input saturation under Assumptions 1–3, if the actual control input (40), the intermediate virtual control signals (16), (28), and the adaptive law (43) are selected, then it can ensure that all states do not exceed asymmetric constraints, and the system output y can track the given reference signal y_d.*

Proof. For the stability analysis of the closed-loop system (1), we define the following asymmetric Lyapunov function

$$V = \sum_{i=1}^{n} \left(\frac{\rho(z_i)}{2} \ln \frac{k_{bi}^2}{k_{bi}^2 - z_i^2} + \frac{1-\rho(z_i)}{2} \ln \frac{k_{ai}^2}{k_{ai}^2 - z_i^2} \right) + \frac{1}{2} \sum_{i=1}^{n} \tilde{\theta}_i^{\mathrm{T}} \tilde{\theta}_i. \tag{46}$$

According to (45), the derivative of V with respect to time t is as follows

$$\dot{V} \leq -\sum_{i=1}^{n} \kappa_i \left(\rho_i \ln \frac{k_{bi}^2}{k_{bi}^2 - z_i^2} + (1-\rho_i) \ln \frac{k_{ai}^2}{k_{ai}^2 - z_i^2} \right) + \sum_{i=1}^{n} \varpi_i \tilde{\theta}_i^{\mathrm{T}} \hat{\theta}_i + \frac{1}{2} \sum_{i=1}^{n} \varepsilon_i^2 + \frac{1}{2} \Delta^2, \tag{47}$$

where κ_i, ϖ_i, Δ and ε_i are positive design parameters.

By the Young's Inequality, the term $\sum_{i=1}^{n} \varpi_i \tilde{\theta}_i^{\mathrm{T}} \hat{\theta}_i$ in (47) can be decomposed as follows

$$\sum_{i=1}^{n} \varpi_i \tilde{\theta}_i^{\mathrm{T}} \hat{\theta}_i \leq -\frac{1}{2} \sum_{i=1}^{n} \varpi_i \tilde{\theta}_i^{\mathrm{T}} \tilde{\theta}_i + \frac{1}{2} \sum_{i=1}^{n} \varpi_i \|\theta_i\|^2. \tag{48}$$

Substituting (48) into (47) leads to

$$\dot{V} \leq -\sum_{i=1}^{n} \kappa_i \left(\rho_i \ln \frac{k_{bi}^2}{k_{bi}^2 - z_i^2} + (1-\rho_i) \ln \frac{k_{ai}^2}{k_{ai}^2 - z_i^2} \right) - \frac{1}{2} \sum_{i=1}^{n} \varpi_i \tilde{\theta}_i^{\mathrm{T}} \tilde{\theta}_i + \frac{1}{2} \sum_{i=1}^{n} \varpi_i \|\theta_i\|^2 + \frac{1}{2} \sum_{i=1}^{n} \varepsilon_i^2 + \frac{1}{2} \Delta^2. \tag{49}$$

Denote $\tau_i = \min\{\kappa_i, \varpi_i\}, i = 1, 2, \ldots, n$, $\tau_0 = \min\{\tau_1, \tau_2, \ldots, \tau_n\}$, and $\bar{h}_0 = \frac{1}{2}\sum_{i=1}^{n} \varpi_i \|\theta_i\|^2 + \frac{1}{2}\sum_{i=1}^{n} \varepsilon_i^2 + \frac{1}{2}\Delta^2$. Then, the inequality (49) can be written as follows

$$\dot{V} \leq -\tau_0 V + \bar{h}_0. \tag{50}$$

From (50), we can get the following inequality

$$0 \leq V(t) \leq \left(V(0) - \frac{\bar{h}_0}{\tau_0} \right) e^{-\tau_0 t} + \frac{\bar{h}_0}{\tau_0}. \tag{51}$$

Because of $\tau_0 > 0$, we can conclude that $V(t)$ is bounded according to inequality (51), and $V(t)$ takes $\frac{\bar{h}_0}{\tau_0}$ as the upper bound. At the same time, all signals of the closed-loop system are bounded. And the tracking error can be arbitrarily small by selecting appropriate design parameters. In addition, since considered variable $z_1 = x_1 - y_d$ satisfies $k_{a1} \leq z_1 \leq k_{b1}$ and $k_{a1} = b_1^- - y_d$, $k_{b1} = b_1^+ - y_d$, then we have $k_{a1} + y_d \leq x_1 \leq k_{b1} + y_d$, that is, $b_1^- \leq x_1 \leq b_1^+$. In the same principle, according to $z_i = x_i - \alpha_{i-1}$, $k_{ai} = b_i^- - Y_{i-1}$, $k_{bi} = b_i^+ - Y_{i-1}$ and $\alpha_{i-1} \leq Y_{i-1}$, we can prove that $b_i^- \leq x_i \leq b_i^+$ for $i = 2, \ldots, n$. Therefore, we can determine that all states are constrained in an asymmetric region.

Remark 7. During the design process, numerous design parameters are involved. According to the previous design and analysis, the tracking performance can be improved by increasing τ_0 or decreasing $\bar{h}_0$. As a result, we can increase τ_0 by increasing κ_i and ϖ_i, and decrease $\bar{h}_0$ by decreasing ϖ_i, ε_i, and Δ. However, as the parameter ϖ_i increases, $\bar{h}_0$ grows larger and larger, and a larger κ_i leads to a larger u. Therefore, the design parameters should be carefully adjusted in practice to achieve appropriate transient performance and control objectives. ∎

4 | SIMULATION STUDIES

The following three simulation examples are given to prove the effectiveness and applicability of the MTN-based control scheme proposed in this paper.

Example 1. Considering the nonlinear system with time-varying full state constraints and input saturation, the description is as follows

$$\begin{cases} \dot{x}_1 = x_2 - x_1 e^{0.5x_1} \\ x_2 = u(v) + 0.5x_1 \cos x_2^2 \\ y = x_1, \end{cases} \tag{52}$$

where x_1 and x_2 are system states with $[x_1(0), x_2(0)]^{\mathrm{T}} = [0, 0]^{\mathrm{T}}$. According to Theorem 1, the control strategy of the system (52) can be designed as $\alpha_1 = -\kappa_1 z_1 - \hat{\theta}_1^{\mathrm{T}} P_{m_1}$, $v = -\frac{1}{\ell^-}\left(\kappa_2 |z_2| + \left|\hat{\theta}_2^{\mathrm{T}} P_{m_2}\right|\right) \mathrm{sgn}(z_2)$ and $\dot{\hat{\theta}}_j = -\varpi_j \hat{\theta}_j + \mu_j z_j P_{m_j}, j = 1, 2$.

In the simulation, the desired tracking signal is selected as $y_d = 0.5 \sin 0.5t$, the asymmetric constraints of states are described as $b_1^- < x_1 < b_1^+$, and $b_2^- < x_2 < b_2^+$, the upper and lower limits are taken as $b_1^- = -0.1 + 0.5 \sin 0.5t$, $b_1^+ = 0.1 + 0.5 \sin 0.5t$, $b_2^- = -0.4 + 0.5 \sin 0.5t$ and $b_2^+ = 0.6 + 0.5 \sin 0.5t$, respectively. Then, the parameters of $u(v)$ are selected as $u_S = 1$ and $u_I = 0.5$. The design parameters are selected as $k_{a1} = -0.5 \sin 0.5t - 0.6$, $k_{b1} = 0.5 \sin 0.5t + 0.6$, $k_{a2} = -0.5 \sin 0.5t - 1.1$, $k_{b2} = 0.5 \sin 0.5t + 1.1$, $\kappa_1 = 20$, $\kappa_2 = 1$, $\ell^- = 1$, $\varpi_1 = 1$, $\varpi_2 = 2$.

The simulation results are shown in Figures 3–7. It can be clearly seen from Figure 3 that the obtained tracking effect is satisfactory, and state x_1 doesn't violate the asymmetric time-varying constraint boundary. Similarly, it can be seen from Figure 4 that the trajectory of x_2 doesn't transgress the constraint boundary. Figures 5–6 describe the trajectory of the controller and the adaptive law, and Figure 7 shows the error trajectory curve. According to the simulation results, it can be seen that all signals of the closed-loop systems are bounded, and the tracking error is controlled in a small neighborhood near the origin, and within the set constraint range, which shows that the designed control strategy is effective and reasonable.

Example 2. In order to further illustrate the feasibility of the scheme, consider the Duffing-Holmes[19] system as follows

$$\begin{cases} \dot{x}_1 = x_2 \\ x_2 = u + x_1 - x_2 - x_1^3 + 0.2 \cos(0.1t) \\ y = x_1, \end{cases} \tag{53}$$

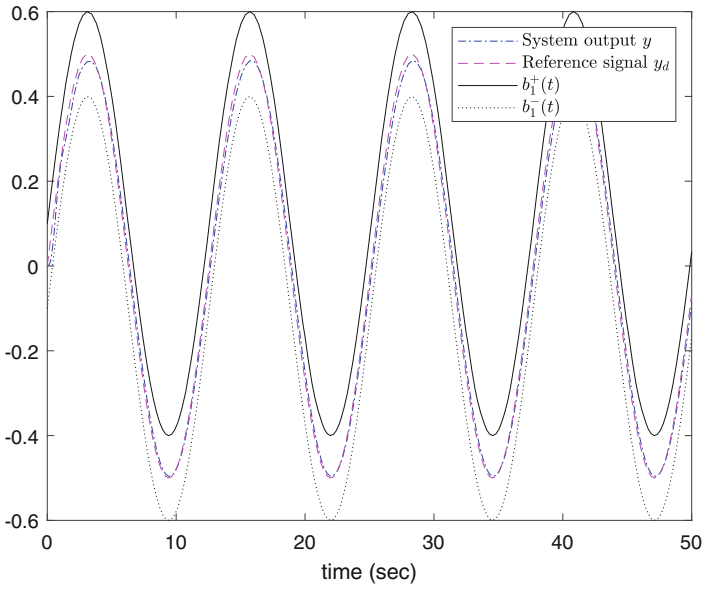

FIGURE 3 The trajectories of y and the tracking signal y_d of system (52)

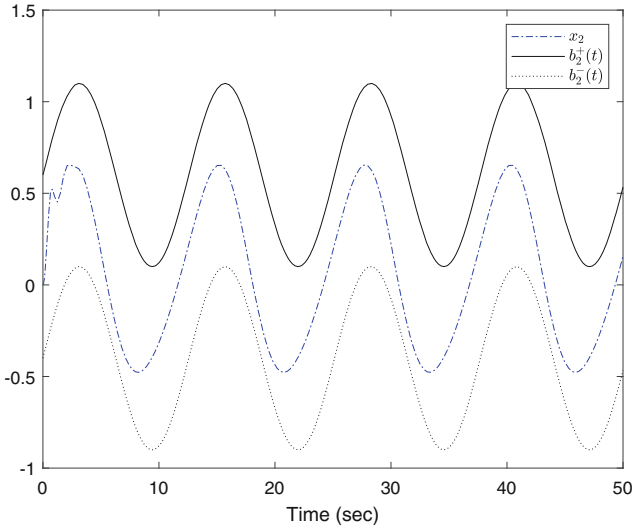

FIGURE 4 Trajectory of state x_2 with constraints

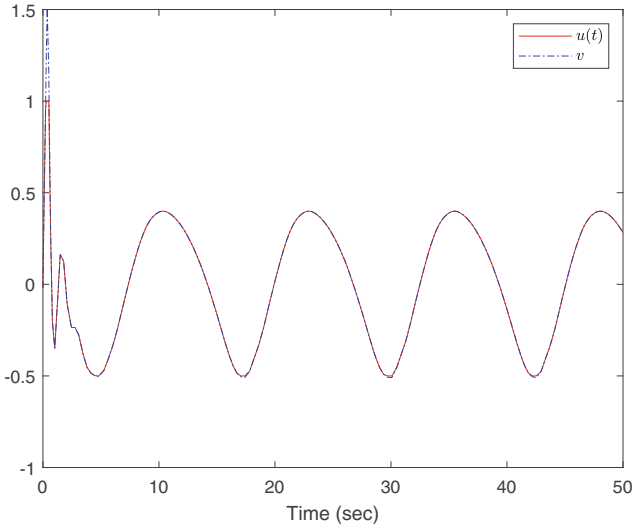

FIGURE 5 Trajectory of control input u of the system

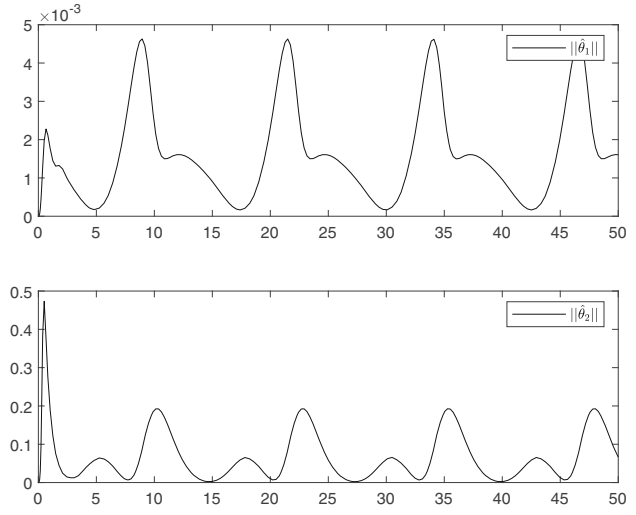

FIGURE 6 The trajectory of the designed adaptive law

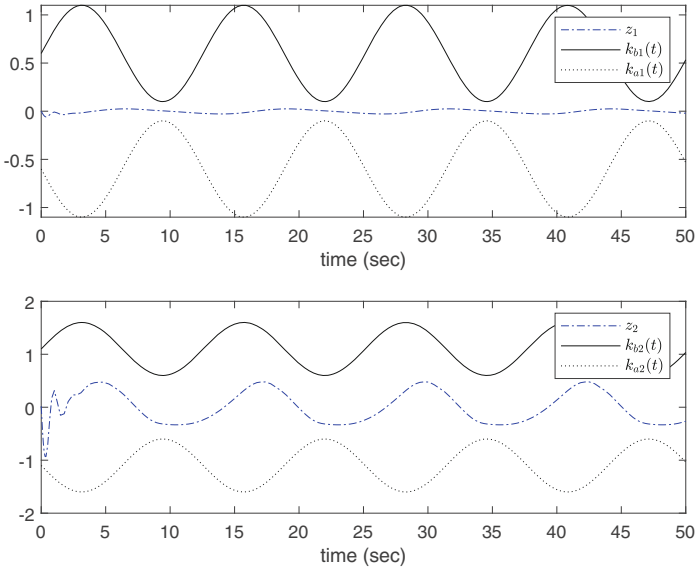

FIGURE 7 Error trajectory with constraints

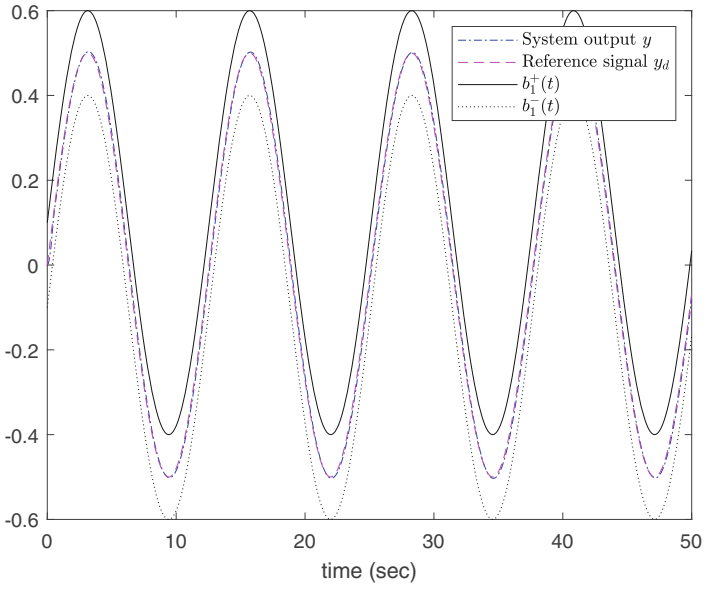

FIGURE 8 The trajectories of output y and the tracking signal y_d of system (53)

where x_1 and x_2 are system states with $[x_1(0), x_2(0)]^{\mathrm{T}} = [0, 0]^{\mathrm{T}}$. According to Theorem1, the control strategy of the system (53) can be designed as $\alpha_1 = -\kappa_1 z_1 - \hat{\theta}_1^{\mathrm{T}} P_{m_1}$, $v = -\frac{1}{\ell^-}\left(\kappa_2 |z_2| + \left|\hat{\theta}_2^{\mathrm{T}} P_{m_2}\right|\right) \mathrm{sgn}(z_2)$ and $\dot{\hat{\theta}}_j = -\varpi_j \hat{\theta}_j + \mu_j z_j P_{m_j}, j = 1, 2$.

In the simulation, the desired tracking signal is selected as $y_d = 0.5 \sin 0.5t$, the asymmetric constraints of states are described as $b_1^- < x_1 < b_1^+$ and $b_2^- < x_2 < b_2^+$, the upper and lower boundaries are taken as $b_1^- = -0.1 + 0.5 \sin 0.5t$, $b_1^+ = 0.1 + 0.5 \sin 0.5t$, $b_2^- = -0.7 + 0.5 \sin 0.5t$ and $b_2^+ = 0.6 + 0.5 \sin 0.5t$, respectively. The parameters of u (v) are selected as $u_S = 1$ and $u_I = -0.8$. Then choose $k_{a1} = -0.5 \sin 0.5t - 0.6$, $k_{b1} = 0.5 \sin 0.5t + 0.6$, $k_{a2} = -0.5 \sin 0.5t - 1.1$, $k_{b2} = 0.5 \sin 0.5t + 1.1$, $\kappa_1 = 20$, $\kappa_2 = 10$, $\ell^- = 1$, $\varpi_1 = 1$ and $\varpi_2 = 2$ as design parameters.

The simulation results are shown in Figures 8-12. It can be clearly seen from the Figure 8 that the output y tracks the desired reference signal y_d, and the tracking effect is gratifying. The full states do not violate the given asymmetric boundary, and the error trajectory converges to a small neighborhood of the origin. The designed controller and adaptive law are also successfully constrained within a certain range. All the above verify the effectiveness and practicability of the control scheme designed in this paper.

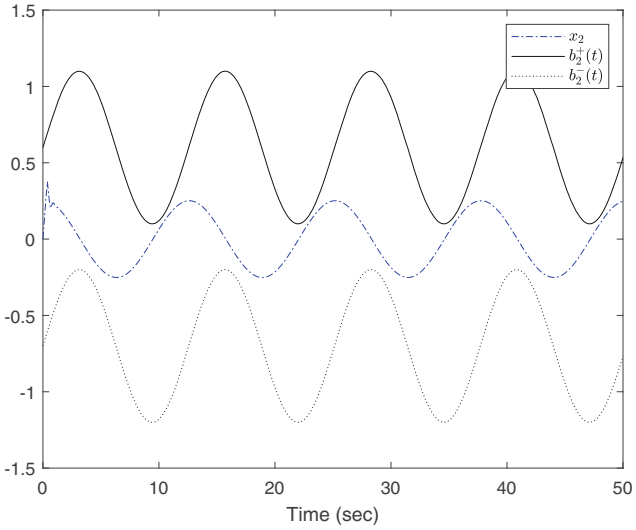

FIGURE 9 Trajectory of state x_2 with constraints

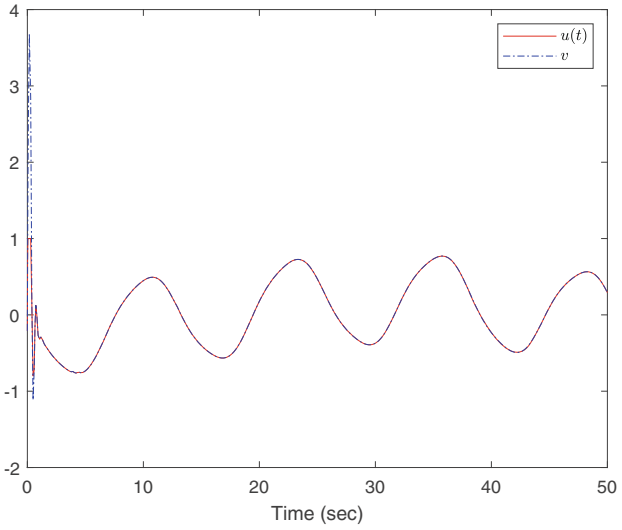

FIGURE 10 Trajectory of control input u of the system

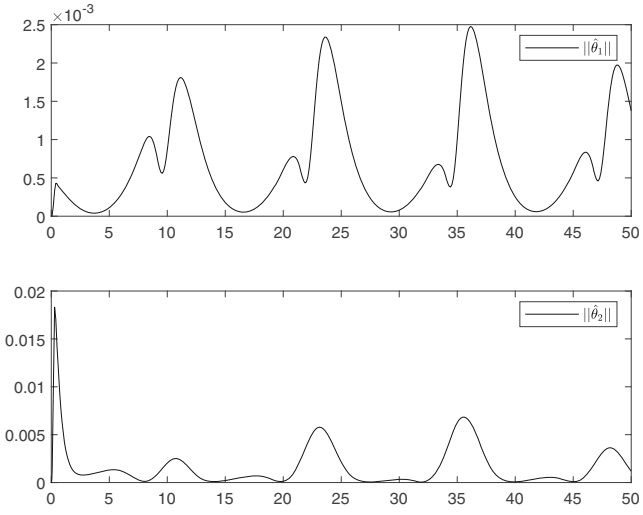

FIGURE 11 The trajectory of the designed adaptive law

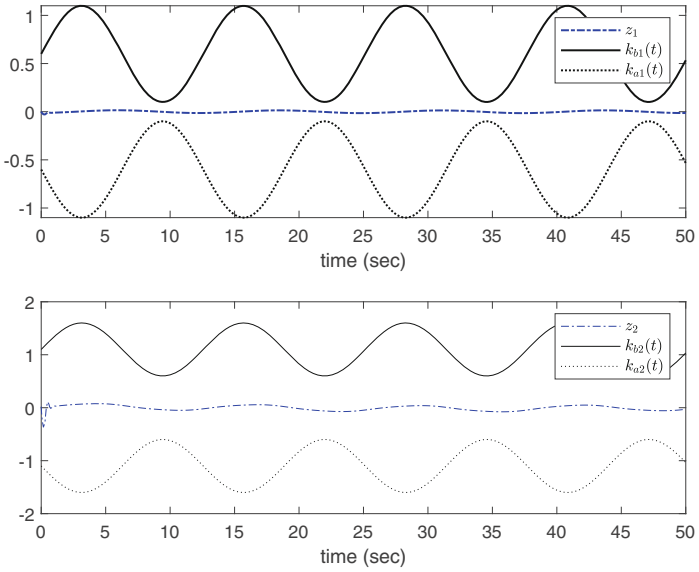

FIGURE 12 The trajectory of error with constraints

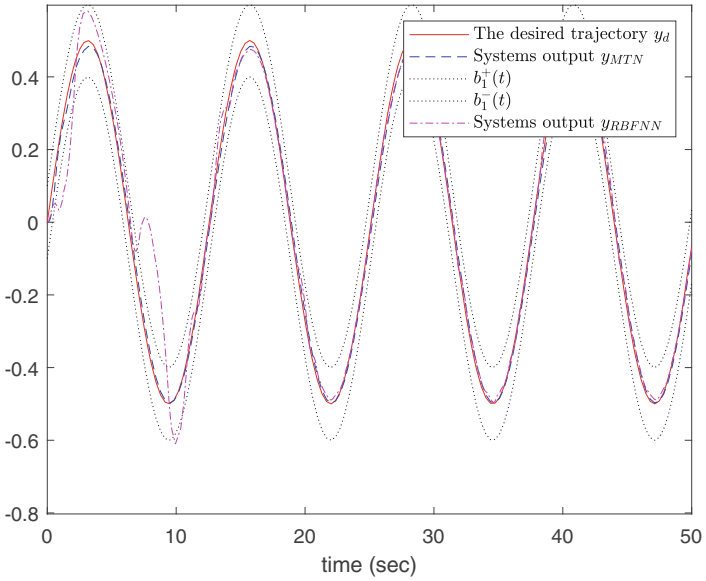

FIGURE 13 Trajectory comparison results of MTN and RBFNN

Remark 8. Simulation result of Examples 1 and 2 shows that, it can be determined that the proposed controller can implement the tracking performance when the control parameters meet $\kappa_i > 0$ and $\varpi_i > 0$. But it is important to note that the above parameters must be appropriately selected for the purpose of achieving the control target and obtain satisfactory control effect.

Example 3 (Comparative experiment). In order to verify the effectiveness of the proposed scheme, in the control structure of Example 1, all MTNs are substituted by radial basis function neural networks (RBFNNs). The simulation result is displayed in Figure 13, where y_d denotes the given reference signal, b_1^+ and b_1^- denote the asymmetric upper and lower boundaries of state x_1, respectively. y_{MTN} and y_{RBFNN} denote the system output based on MTN method and RBFNN method, respectively.

As illustrated in Figure 13, both MTN-based controller and RBFNN-based controller can implement the tracking control of the desired reference signal. However, the former can guarantee that no state exceeds the given asymmetry

constraint, whereas the latter cannot. As a result, we can conclude that the former has a better control effect than the latter. Furthermore, compared to RBFNN, MTN has a simpler structure and lower complexity. Therefore, the control approach proposed in this article offers adequate control at a low cost.

5 | CONCLUSION

A MTN adaptive tracking control scheme has been developed for a class of nonlinear systems with asymmetric time-varying full state constraints and input saturation. With the help of auxiliary function, the influence of system input saturation is eliminated to a certain extent. The time-varying ABLFs are selected as candidate Lyapunov functions to control the system state variables to fall within the asymmetric constraint range. In the controller design, the MTN control technology is integrated into the backstepping process, and the MTN structure is used to approximate the nonlinear function to construct a simple tracking controller. The proposed scheme ensures that all state variables do not violate the time-varying constraints, all signals of the closed-loop system are bounded, and a good tracking effect is obtained.

It should be noted that the output constraints and the stochastic disturbance frequently during the process of control system, and how to eliminate the negative effects of output constraints and the stochastic disturbance is of great significance. Therefore, our future research will be devoted to handle such a problem for nonlinear systems with asymmetric time-varying full state constrained based on the proposed MTN-based approch.

ORCID

Na Li https://orcid.org/0000-0002-7911-8903
Wen-Jing He https://orcid.org/0000-0001-6370-592X
Yu-Qun Han https://orcid.org/0000-0002-9055-2954

REFERENCES

1. Rehan M, Hong KS, Ge SS. Stabilization and tracking control for a class of nonlinear systems. *Nonlinear Anal Real World Appl*. 2011;12(3):1786-1796.
2. Fan B, Yang QM, Jagannathan S, Sun YX. Asymptotic tracking controller design for nonlinear systems with guaranteed performance. *IEEE Trans Cybern*. 2018;48(7):2001-2011.
3. Yang D, Zong GD, Nguang SK, Zhao XD. Bumpless transfer H_∞ anti-disturbance control of switching Markovian LPV systems under the hybrid switching. *IEEE Trans Cybern*. 2022;52(5):2833-2845.
4. Tong SC, Li YM. Adaptive fuzzy output feedback tracking backstepping control of strict-feedback nonlinear systems with unknown dead zones. *IEEE Trans Fuzzy Syst*. 2012;20(1):168-180.
5. Wang YJ, Lin W. Semiglobal asymptotic stabilization of nonlinear systems with triangular zero dynamics by linear feedback. *Automatica*. 2020;115:108870.
6. Zong GD, Sun HB, Nguang SK. Decentralized adaptive neuro-output feedback saturated control for INS and its application to AUV. *IEEE Trans Neural Networks Learn Syst*. 2021;32(12):5492-5501.
7. Tong DB, Xu C, Chen QY, Zhou WN. Sliding mode control of a class of nonlinear systems. *J Franklin Inst*. 2020;357(3):1560-1581.
8. Liu ZC, Dong XM, Xue JP, Zhang LP. Adaptive tracking control for nonlinear systems with a class of input nonlinearities. *Asian J Control*. 2016;18(2):771-778.
9. Li DJ, Li J, Li S. Adaptive control of nonlinear systems with full state constraints using integral barrier Lyapunov functionals. *Neurocomputing*. 2016;186:90-96.
10. Lu CX, Pan YN, Liu Y, Li HY. Adaptive fuzzy finite-time fault-tolerant control of nonlinear systems with state constraints and input quantization. *Int J Adapt Control Signal Process*. 2020;34(9):1199-1219.
11. Zong GD, Yang D, Lam J, Song XQ. Fault-tolerant control of switched LPV systems: a bumpless transfer approach. *IEEE/ASME Trans Mechatron*. 2022;27(3):1436-1446.
12. Hua CC, Liu PX, Guan XP. Backstepping control for nonlinear systems with time delays and applications to chemical reactor systems. *IEEE Trans Ind Electron*. 2009;56(9):3723-3732.
13. Ding BC, Sun HX, Yang P. Further studies on LMI-based relaxed stabilization conditions for nonlinear systems in Takagi-Sugeno's form. *Automatica*. 2006;42(3):503-508.
14. Ge SS, Zhang J, Lee TH. Adaptive neural network control for a class of MIMO nonlinear systems with disturbances in discrete-time. *IEEE Trans Syst Man Cybern B Cybern*. 2004;34(4):1630-1645.
15. Ge SS, Hong F, Lee TH. Adaptive neural network control of nonlinear systems with unknown time delays. *IEEE Trans Automat Control*. 2003;48(11):2004-2010.
16. Jia C, Li XL, Wang K, Ding DW. Adaptive control of nonlinear system using online error minimum neural networks. *ISA Trans*. 2016;65:125-132.

17. Zhao XD, Wang XY, Zong GD, Li HM. Fuzzy-approximation-based adaptive output-feedback control for uncertain nonsmooth nonlinear systems. *IEEE Trans Fuzzy Syst*. 2018;26(6):3847-3859.
18. Niu B, Liu LN, Liu YY. Adaptive backstepping-based fuzzy tracking control scheme for output-constrained nonlinear switched lower triangular systems with time-delays. *Neurocomputing*. 2016;175:759-767.
19. Yang YL, Gao WN, Modares H, Xu CZ. Robust actor-critic learning for continuous-time nonlinear systems with unmodeled dynamics. *IEEE Trans Fuzzy Syst*. 2022;30(6):2101-2112.
20. Chen M, Wang HQ, Liu XP. Adaptive fuzzy practical fixed-time tracking control of nonlinear systems. *IEEE Trans Fuzzy Syst*. 2021;29(3):664-673.
21. Han YQ, Zhu SL, Yang SG, Chu L. Adaptive multi-dimensional Taylor network tracking control for a class of nonlinear systems. *Int J Control*. 2021;94(2):277-285.
22. Chu L, Han YQ, Zhu SL, Wang MX. Multi-dimensional Taylor network-based adaptive control for nonlinear systems with unknown parameters. *Trans Ins Meas Control*. 2021;43(3):646-655.
23. Yan HS, Sun QM, Zhou B. Multidimensional Taylor network optimal control of SISO nonlinear systems for tracking by output feedback. *Optim Control Appl Methods*. 2018;39(2):919-932.
24. Sun QM, Yan HS. Multi-dimensional Taylor network modelling and optimal control of SISO nonlinear systems for tracking by output feedback. *IMA J Math Control Info*. 2020;37(3):699-717.
25. Sun QM, Yan HS. Multidimensional Taylor network optimal control of MIMO nonlinear systems without models for tracking by output feedback. *Math Probl Eng*. 2017;2017:1548095.
26. Zhang C, Yan HS. Multi-dimensional Taylor network adaptive control for MIMO time-varying uncertain nonlinear systems with noises. *Int J Robust Nonlinear Control*. 2020;30(1):397-420.
27. Han YQ, He WJ, Li N, Zhu SL. Adaptive tracking control of a class of nonlinear systems with input delay and dynamic uncertainties using multi-dimensional Taylor network. *Int J Control Automat Syst*. 2021;19:4078-4089.
28. Min HF, Xu SY, Zhang ZQ. Adaptive finite-time stabilization of stochastic nonlinear systems subject to full-state constraints and input saturation. *IEEE Trans Automat Control*. 2021;66(3):1306-1313.
29. Li DJ, Li DP. Adaptive tracking control for nonlinear time-varying delay systems with full state constraints and unknown control coefficients. *Automatica*. 2018;93:444-453.
30. Han YQ. Adaptive control of a class of stochastic nonlinear systems with full state constraints and input saturation using multi-dimensional Taylor network. *Asian J Control*. 2022;24(4):1609-1621.
31. Zhang JJ. Adaptive multi-dimensional Taylor network dynamic surface control for a class of strict-feedback uncertain nonlinear systems with unmodeled dynamics and output constraint. *ISA Trans*. 2021;108:35-47.
32. Gao TT, Liu YJ, Liu L, Li DP. Adaptive neural network-based control for a class of nonlinear pure-feedback systems with time-varying full state constraints. *IEEE/CAA J Automat Sinica*. 2018;5(5):923-933.
33. Gao TT, Liu YJ, Li DP, Tong SC, Li TS. Adaptive neural control using tangent time-varying BLFs for a class of uncertain stochastic nonlinear systems with full state constraints. *IEEE Trans Cybern*. 2021;51(4):1943-1953.
34. Lan J, Liu YJ, Liu L, Tong SC. Adaptive output feedback tracking control for a class of nonlinear time-varying state constrained systems with fuzzy dead-zone input. *IEEE Trans Fuzzy Syst*. 2021;29(7):1841-1852.
35. Liu YJ, Ma L, Liu L, Tong SC, Chen CLP. Adaptive neural network learning controller design for a class of nonlinear systems with time-varying state constraints. *IEEE Trans Neural Networks Learn Syst*. 2020;31(1):66-75.
36. Wang CX, Wu YQ, Yu JB. Barrier Lyapunov functions-based adaptive control for nonlinear pure-feedback systems with time-varying full state constraints. *Int J Control Automat Syst*. 2017;15(6):2714-2722.
37. Liu L, Gao TT, Liu YJ, Tong SC. Time-varying asymmetrical BLFs based adaptive finite-time neural control of nonlinear systems with full state constraints. *IEEE/CAA J Automat Sinica*. 2020;7(5):1335-1343.
38. Lin D, Wang XY, Yao Y. Fuzzy neural adaptive tracking control of unknown chaotic systems with input saturation. *Nonlinear Dyn*. 2012;67(4):2889-2897.
39. Chen M, Ge SS, Ren BB. Adaptive tracking control of uncertain MIMO nonlinear systems with input constraints. *Automatica*. 2011;47(3):452-465.
40. Wen CY, Zhou J, Liu ZT, Su HY. Robust adaptive control of uncertain nonlinear systems in the presence of input saturation and external disturbance. *IEEE Trans Automat Control*. 2011;56(7):1672-1678.
41. Wang HQ, Chen B, Liu XP, Liu KF, Lin C. Adaptive neural tracking control for stochastic nonlinear strict-feedback systems with unknown input saturation. *Inform Sci*. 2014;269:300-315.
42. Wang CH, Cui LM, Liang M, Li JL, Wang YT. Adaptive neural network control for a class of fractional-order nonstrict-feedback nonlinear systems with full-state constraints and input saturation. *IEEE Trans Neural Networks Learn Syst*. 2021. doi:10.1109/TNNLS.2021.3082984
43. Zhou Q, Li HY, Wu CW, Wang LJ, Ahn CK. Adaptive fuzzy control of nonlinear systems with unmodeled dynamics and input saturation using small-gain approach. *IEEE Trans Syst Man Cybern Syst*. 2017;47(8):1979-1989.
44. Li YM, Tong SC, Li TS. Adaptive fuzzy output-feedback control for output constrained nonlinear systems in the presence of input saturation. *Fuzzy Set Syst*. 2014;248:138-155.
45. Chen ZT, Li ZJ, Chen CLP. Adaptive neural control of uncertain MIMO nonlinear systems with state and input constraints. *IEEE Trans Neural Networks Learn Syst*. 2017;28(6):1318-1330.
46. Yang YL, Ding DW, Xiong HY, Yin YX, Wunsch DC. Online barrier-actor-critic learning for H∞ control with full-state constraints and input saturation. *J Franklin Inst*. 2020;357(6):3316-3344.

47. Wang YD, Zong GD, Yang D, Shi KB. Finite-time adaptive tracking control for a class of nonstrict feedback nonlinear systems with full state constraints. *Int J Robust Nonlinear Control*. 2022;32(5):2551-2569.
48. Han YQ, Li N, He WJ, Zhu SL. Adaptive multi-dimensional Taylor network funnel control of a class of nonlinear systems with asymmetric input saturation. *Int J Adapt Control Signal Process*. 2021;35(5):713-726.
49. Zhu SL, Han YQ. Adaptive decentralized prescribed performance control for a class of large-scale nonlinear systems subject to nonsymmetric input saturation. *Neural Comput Appl*. 2022;34(13):11123-11140.
50. Yang YL, Liu ZJ, Li Q, Wunsch DC. Output constrained adaptive controller design for nonlinear saturation systems. *IEEE/CAA J Automat Sinica*. 2021;8(2):441-454.
51. Zong GD, Wang YD, Karimi HR, Shi KB. Observer-based adaptive neural tracking control for a class of nonlinear systems with prescribed performance and input dead-zone constraints. *Neural Networks*. 2022;147:126-135.
52. Ma JJ, Ge SS, Zheng ZQ, Hu DW. Adaptive NN control of a class of nonlinear systems with asymmetric saturation actuators. *IEEE Trans Neural Networks Learn Syst*. 2015;26(7):1532-1538.
53. Yu ZX, Dong Y, Li SG, Li FF. Adaptive tracking control for switched strict-feedback nonlinear systems with time-varying delays and asymmetric saturation actuators. *Neurocomputing*. 2017;238:245-254.
54. Lin Y, Yan HS, Zhou B. Nonlinear time series prediction method based on multi-dimensional Taylor network and its applications. *Control Decis*. 2014;29(5):795-801.

How to cite this article: Li N, Zhu S-L, He W-J, Han Y-Q. Controller design for nonlinear systems subject to both input saturation and asymmetry time-varying state constraints: A novel network-based approach. *Int J Adapt Control Signal Process*. 2022;36(12):3124-3141. doi: 10.1002/acs.3503